Validation Report

Name of Report	A comparison of OmniSim's FDDT engine and subgridding technique with published data
Performance Date	December 2006
Performed By	Klearchos Chaloulos
Product Name	OmniSim
Product Version & Compile Date	Version: 4.1, Compiled: 3rd December 2006
References	K. B. Crozier,a) A. Sundaramurthy, G. S. Kino, and C. F. Quate, "Optical antennas: Resonators for local field enhancement", Journal of Applied Physics, Vol. 94, Number 7, 2003
External Files	OpticalAntennas.prj

A comparison of OmniSim's FDDT engine and subgridding technique with published data

08/12/2006

Abstract

We evaluated the extinction cross section of gold optical antennas on a silicon substrate. The results were compared with Crozier et al [1], and were found to be very close to both the experimental and simulation data in that paper. The simulations were repeated using the sub-gridding technique, with excellent agreement.

Definitions

The extinction cross section is usually defined by the equation:

$$P_{out} = P_{in} - C_{ext} \cdot I_{in} \qquad (1)$$

where P_{out} and P_{in} are the output and input powers (Watts), I_{in} is the incident intensity (W/m^2) and C_{ext} is the extinction cross section (m^2). It should be noted that the power P_{out} has to be power propagating only in the direction of the excitation. For an incident plane wave, it is $I_{in}=P_{in}/A$, where A is the area of our structure. Then we can rewrite (1) as:

$$C_{ext} = A \cdot \left(1 - \frac{P_{out}}{P_{in}}\right) \qquad (2)$$

The definition of the extinction cross section can become more ambiguous when there is more tht one element in the structure. For instance, in [1] the structure consists of a golden antenna on a silicon substrate. Obviously the Fresnel reflection on the silicon-air interface will influence the power transmission. However, this reflection is not a characteristic of the golden antenna. In that case, we can take that into account by defining the extinction cross section from the equation:

$$P_{out} = P_{in} - C_{ext} \cdot I_{in} - R_{Fresnel}(A - C_{ext}) \cdot I_{in} \qquad (3)$$

The definition of Eq. 3 has the advantage, in this specific case, that in the absence of the antenna, where C_{ext} has to be equal to zero, (3) gives us the correct transmitted power. It also gives $P_{out}=P_{in}$ for $C_{ext}=A$. If we solve for C_{ext} we get:

$$C_{ext} = A \cdot \left(1 - \frac{P_{out}}{T_{Fresnel} P_{in}}\right) \qquad (4)$$

We must note that Pout should represent only the flux travelling in the same direction as the incident wave. This can be evaluated by an overlap integral of the form

$$c = \int \left(E_z^{out} H_x^{in} - E_x^{out} H_z^{in}\right) dxdz \qquad (5),$$

for a wave travelling along the y-direction. The power is then given by c^2, if the H's are normalised for an incident power of 1.

Constructing the structure

The first thing to do when constructing the structure is to grow the physical layers. We chose the thicknesses and materials shown on Fig. 1. For the Antenna layer, the Etch&Fill mechanism was used, with the Inverse property of the mask layer set to "True", so that the drawn shape would not be etched. The fill material was set to be gold.

Figure 1: Physical Layers showing thicknesses and materials used for the simulation

The mask layer can be seen on Fig. 2, for the four geometries considered. The dimensions are set to be the same as the ones report in [1], in the extinction cross section experiments. The geometry of the structure was studied, and the "Variables" option of OmniSim was used, so that the coordinates of each constituting would be automatically calculated. The goal was that all shapes would exactly match for example the straight lines of the taper section (middle of the shape), would be tangential to all the circles at the edges. Thanks to the "Variables" tool (Fig. 2), we can insert the input parameters, like length, tip angle and radius of curvature at the tips, and immediately get the antenna. The detailed dimensions of the antennas can be seen on Table 1.

	Length (um)	Tip Angle (degrees)	Tip Radius (nm)	Width (um)
Linear	1.55	-	120	0.12
30 deg	1.56	30	0.14	-
60 deg	1.56	60	0.19	-
Circular	1.7	-	-	1.5

Table 1: Geometrical dimensions of the antennas, used as input parameters for the variables window.

The materials referenced (Si, Au) were fitted from Photon Design's database, with a 10% tolerance over the wavelength range 6-16um. The central wavelength of the FDDT calculation was 10.375um. The excitation was a sinusoidal pulse with 6um nominal bandwidth around 10.375um, a plane wave travelling along the y-axis. The end section view (x-y) of the structure for the linear antenna case can be seen on Fig. 4.

The device x and y dimensions was 3x3um. With the x and y boundary conditions set to periodic, this simulates an array of antennas spaced by 3um in each direction, as described in [1].

Variables: ShapeCoordinates

File Edit

Name	Expression	Value
Lnom	1.56	1.56
ThetaDegHalfAngle	15	15
R	0.14	0.14
BoxLength	3	3
Theta	ThetaDegHalfAngle*3.14/180	0.26166667
d	R/sin(Theta)-R	0.40118653
L	Lnom	1.56
ds	R*(1-sin(Theta))	0.10378328
dss	R*sin(Theta)	0.036216718
d1	dss	0.036216718
ws	(R+d1)*tan(Theta)	0.047192061
W	2*(L+d)*tan(Theta)	1.0504388
Lc	L-ds-R-d1	1.28
w2	2*R*cos(Theta)	0.27046885
Wc	W-2*ws	0.95605463
Phi	(1.57-Theta)/2	0.65416667
h1	R/tan(Phi)	0.18257695
wm	W/2-h1	0.34264242
TaperZPos	-L/2+R+d1	-0.60378328
CircleTipZPosCentre	Lc-dss+TaperZPos	0.64
CirclesZPosCentre	TaperZPos-d1	-0.64
CirclesXPosCentre	wm	0.34264242
RectLength	R+d1	0.17621672
RectWidth	2*wm	0.68528485
RectZPos	TaperZPos-d1-R+RectLength/2	-0.69189164

Figure 2: Variables window

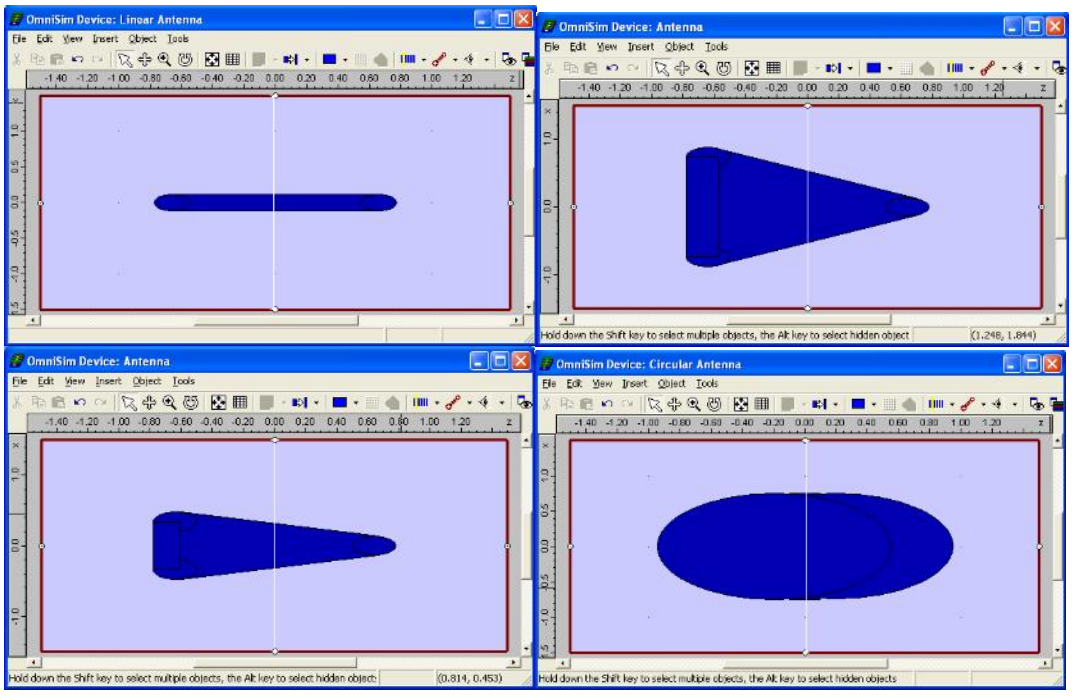

Figure 3: Mask layer showing the shape of each of the four antennas: Linear (top left), equilateral triangular with tip angle 60^{o} (top right), isosceles triangular with tip angle 30^{o} (bottom left) and circular (bottom right). The red rectangle is the Output sensor.

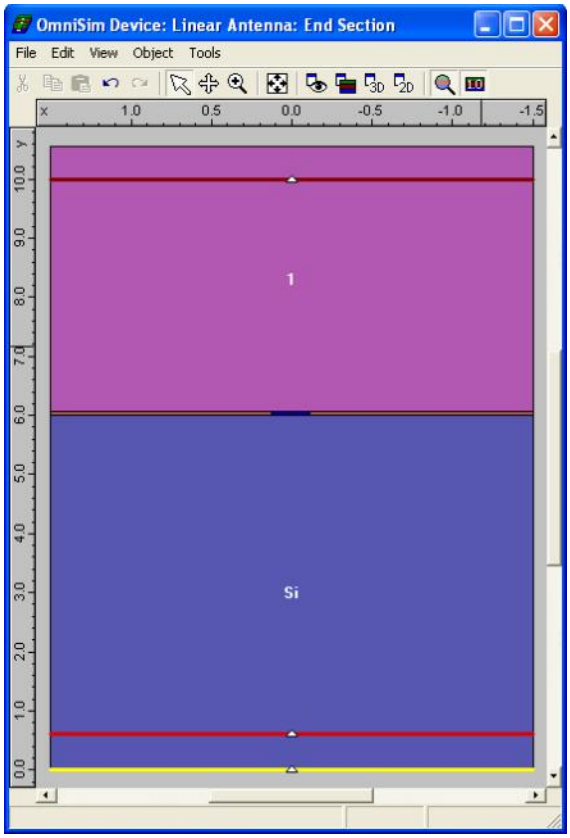

Figure 4: End section (x-y) view of the device. The golden antenna is the blue rectangle in the centre. The beam excitor is the yellow line, located at the bottom of the device. We can see the two sensors, the Reference (bright red near the bottom) and the Output (darker red near the top).

To calculate the cross section we can apply Eq. 4. The ratio P_{out}/P_{in} is readily the plot of the positive flux through the output over the positive flux though the reference sensor. The Fresnel transmission coefficient is 0.993 for a refractive index of silicon 3.4766 is 0.6939. Strictly speaking, the output flux must be calculated for an integral of the form of Eq. 5. However, as explained in [1], the experimental setup collects power through a finite solid angle, but as most power is radiated into the substrate, the results are expected to be accurate. In our simulation, if we place the sensors away enough from the antenna, so that they are outside the immediate oscillating field around it, the field is practically flat, as we see on Fig. 5. Therefore it wouldn't make any appreciable difference to the integral. We plot the intensity vs position at 10.375um, a near-resonance wavelength, so that it shows the form of the re-radiated power. The fact that the field at the sensors is almost flat is also a good indication that the positive and negative flux calculated at the sensors is accurate. OmniSim sensors suffer from a limitation that thy might yield inaccurate results for the positive and negative flux through them, if there is a significant amount of power travelling at angles $>45^{o}$ to the direction normal to the sensor. The net flux is always accurate.

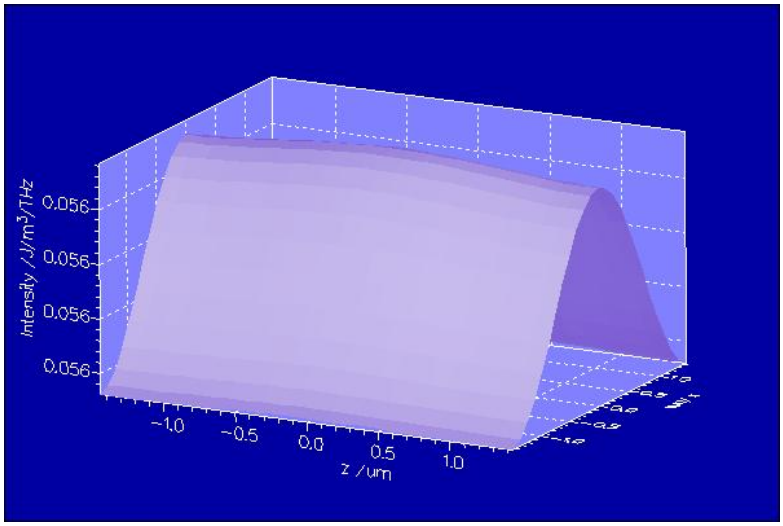

Figure 5: Intensity vs position at the output sensor, step 25000. Note that the vertical axis is constant at 0.56 J/(m^2THz). Plotted for 10.375 um.

Results

We did two kinds of simulations, one with a uniform grid along the whole structure, and one using the feature of subgridding. For the uniform grid, we used a grid spacing of 30nm. For the subgridding, we used a major grid spacing of 120nm, and an 8x subgriding around the antenna. That means that around the antenna the grid spacing was 15nm. Subgridding region extended for 3 major grid cells (0.36um) around the antenna. Apart from the subgridding the only difference between the two types of simulation was that the no-subgrid one covered a longer time (6864fs instead of 715fs). However this is not expected to introduce any difference, as the fields and currents in the antenna have already practically reached zero by the 715fs. Good proof for that is the very good agreement between the simulation s with and without subgridding. Longer simulations with the subgridding could lead to numerical instabilities.

We see the results of the simulations on Fig. 6, superimposed with the results from [1]. We see very good agreement in the cases of the 30 and 60 degrees triangular antennas. There is a small deviation in the case of the circular antenna, for wavelengths longer than 10um, where the OmniSim simulation predicts a higher extinction cross section, although the trend is the same. This difference could be attributed to differences in the geometry of the circular antenna, as not all dimensions are defined unambiguously in [1].

Bigger differences can be observed in the case of the linear antenna. We note that this is the case where the biggest differences between the experiment and FDTD simulations can be observed. The main reason should be the high field concentration at the small area around the tips of the antenna, and the small antenna dimensions. This causes difficulties in constructing the FDTD grid and accurately representing the field. However, we should mention that the resonance wavelength from OmniSim is between the experimental and simulation results from [1]. The same is true for the extinction cross section for wavelengths bigger than the resonance wavelength, where our line lies between the experiment and simulation lines from [1].

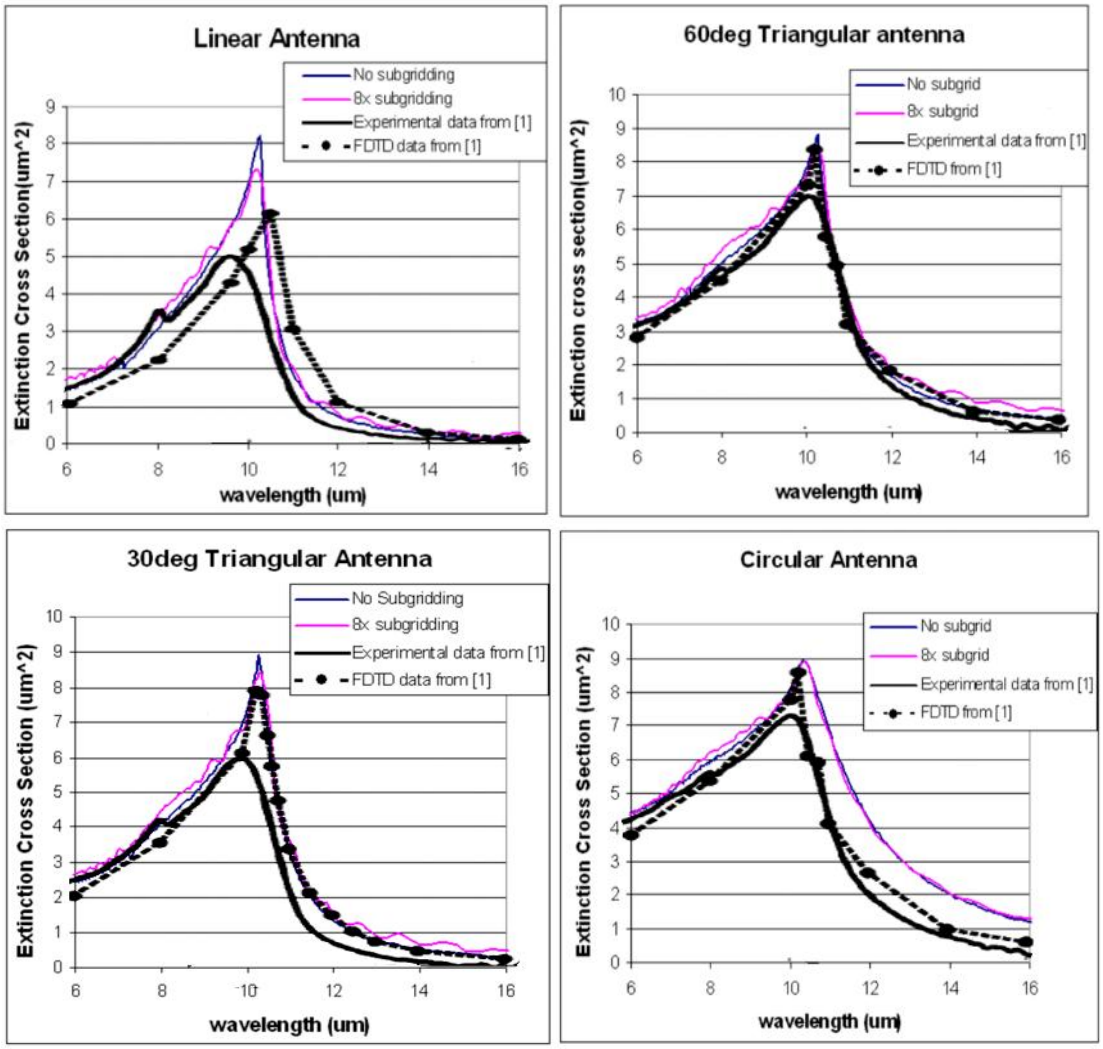

Figure 6: Extinction cross section graphs. Blue (No subgridding) and magenta (8x subgridding) lines come from our OmniSim simulation. Solid black (experimental) and dashed black (FDTD) come from [1]

Another possible source of difference is the way the materials were modelled. OmniSim modelled Si with a static model of dielectric constant vs wavelength, while gold was modelled with a Drude model with a collision frequency of 114.89941THZ and plasma frequency of 14410.472. The resulting fit was within 10% of the experimental data for the complex dielectric constant of gold over the wavelength range from 6 to 16um. A plot can be seen on Fig. 7.

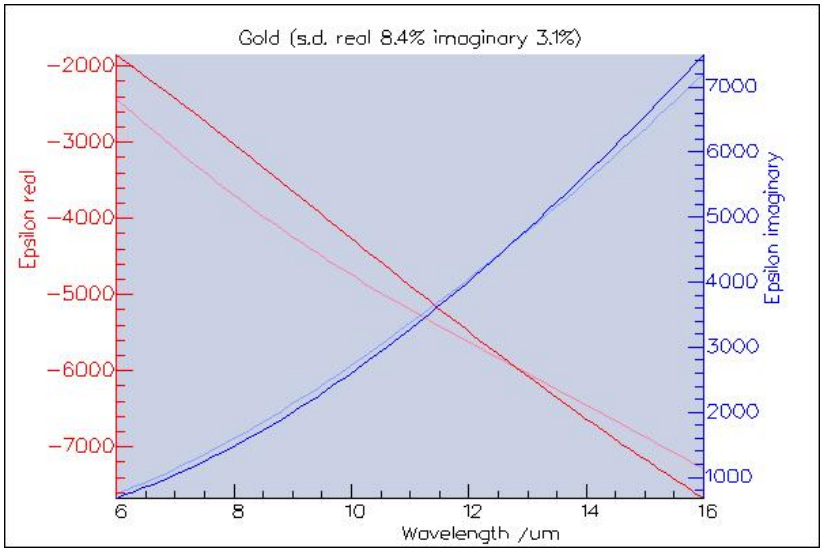

Figure 7: Plot of the complex dielectric constant of gold vs wavelength. The red lines represent the real part and the blue the imaginary. The dark lines are the reference data, while the lighet ones show OmniSim's fit.

Conclusion

In this report we tried to reproduce the results obtained for the extinction cross section of golden optical antennas in [1]. We discussed the definition of the extinction cross section, and described in detail the geometry, materials and FDTD parameters of the simulated structures. We found good agreement between the results from OmniSim and the results from [1]. We also tested the subgridding technique, with the agreement between the normal simulations and the simulations with subgridding being excellent.

Reference:

[1] K. B. Crozier,a) A. Sundaramurthy, G. S. Kino, and C. F. Quate, "Optical antennas: Resonators for local field enhancement", Journal of Applied Physics, Vol. 94, Number 7, 2003